SSRG International Journal of Electrical and Electronics Engineering
ISSN: 2348 – 8379 / https://doi.org/10.14445/23488379/IJEEE-V9I8P102

Volume 9 Issue 8, 8-16, August 2022

Original Article

New Hybrid Cuk-Landsman High Gain Dc-Dc Converter Modelling and Analysis

P. Deepa[1], S. Rajakumar[2], P. Josephin Shermila[3], E. Anna Devi[4], M. Eugine Prince[5], A. Jasmine Gnana Malar[6]

[1]*Department of Electronics & Instrumentation Engineering, St.Joseph's college of engineering, Chennai, Tamil Nadu, India..*
[2] *Department of Electronics and Communication Engineering, Panimalar Engineering College, Chennai, Tamil Nadu, India.*
[3]*Artificial Intelligence and Data Science, R. M. K. College of Engineering and Technology, Thiruvallur District, Tamilnadu, India.*
[4]*Department of Electronics and Communication Engineering, Sathyabama Institute of Science and Technology, Chennai, Tamil Nadu, India.*
[5]*Department of Physics, S.T.Hindu College, Nagercoil, Tamilnadu, India*
[6]*Department of Electrical and Electronics Engineering, PSN College of Engineering and Technology, Tirunelveli, Tamil Nadu, India*

[1]*deepakumaran2002@gmail.com*

Received: 13 June 2022 Revised: 10 August 2022 Accepted: 16 August 2022 Published: 31 August 2022

Abstract - *Due to the rising adoption of energy sources, the requirement for DC-DC converters has increased. As solar source's low voltage, high gain boost converters are necessary for distributed photovoltaic production systems. The converter is created thus for the drawbacks of being larger and less efficient. This research proposes a novel hybrid Cuk and Landsman converter (HCLC) designed to obtain a higher voltage conversion ratio, better efficiency, and reduced driver circuits. The proposed converter is considering the use of a soft switching technique of the switches to reduce the current and voltage. Due to the obvious constant source current, the developed converter achieves low input current stress. MATLAB-Simulink is used to model the proposed work. To assess the effectiveness of the suggested structure, extensive comparisons and replication data are offered.*

Keywords - *DC-DC converter with High Voltage, Cuk Converter, Landsman Converter, PV Power, Buck-Boost.*

1. Introduction

Renewable energy usage for power production is growing daily, and solar photovoltaic power generation, in particular, is essential for creating electricity. The converter is essential to the overall plant in any energy generation and transmission. This research focused on the DC-DC converter in Solar Power generation to maintain continuous input and output with high gain. The converter offers high gain, less current, and voltages on switches and diodes by using Active-Passive inductor cells. While the discontinuous conduction mode (DCM) only employs the partial inductor supply mode, the suggested Continuous conduction mode (CCM) operates in both complete and incomplete inductor supply modes [1].

Microgrids can be maintained using renewable energy sources like fuel cells, solar photovoltaics, etc., by using a DC-DC converter of a voltage multiplier cell [2]. A comparative analysis of duty ratios based on voltage gain and efficiency was conducted. The converter provides 93.6% of the efficiency suggested for microgrids [3]. Soft switching interleaved boost techniques are used in the design of the PV system architecture to achieve high gain medium voltage dc buses. As a result, the converter improves its power rating; it provides a direct connection to the medium voltage dc bus and grid [4].

Using a two-level boost-buck converter is suggested as the repair for the transformer-less DC-DC converter adopted for fuel cell applications. In contrast to the conventional approach, synchronous rectifiers increase the converter's efficiency by 5% [5][6]. A solar photovoltaic system with a fixed step is controlled by a predictive control law to step the Incremental Conductance (INC) under varying sun illumination.[23] According to the implementation, INC MPPT outperforms the other method compared to model predictions [20]. For the fuel cell application, the system should attain high gain, high efficiency, and high response, so the conventional converter is insufficient to meet the requirements. Hence, this application implements the capacitor and switched inductor method [9].

Several passive components, such as diodes, inductors, and capacitors, can be used to generate potential voltage-step-up switching cells. Short circuits can also be substituted for passive components. With non-isolated power electronics circuits, these cells provide high DC gains via boost converters [10]. It is possible to replace the branches with diodes, inductors, capacitors, shorts, and open-circuits with a hybrid non-isolated boost converter (ZETA, SEPIC, Cuk, buck-boost, boost), which incorporates switching diodes, capacitors, and inducers into a fundamental power stage. [11] The quadratic Boost converter is the least stressed in voltage and current stress. Also, the quadratic Boost converter doesn't suddenly change in inductor currents and capacitor voltages during switching, so storage components are not immediately over voltage or over current, and input currents aren't pulsating, simplifying the design of input filters.

This paper presents an innovative hybrid Cuk-Landsman DC-DC converter architecture. The proposed converter contributes significantly by maximizing voltage conversion ratios, improving efficiency, and reducing driver circuitry. Additionally, the output voltage will be stabilized. As described in section 2, the Cuk and Landsman converters are described in the following format. The proposed converter design is discussed in section 3. A mathematical model is derived for the suggested converter in section 4. The proposed strategy is evaluated according to its simulated outcomes and performance in section 5. In sector 6, you will find the answer.

2. Landsman and Cuk Converter

The Cuk converter is the voltage regulator in various DC source applications. It works with different input sources, which means the hybrid of various energy systems like Solar, Wind, Fuel cell, etc. Because it employed straightforward L-C filters, the inductor had less peak-to-peak ripple current than a buck-boost converter. The Cuk converter, which adds an extra inductor and capacitor to store energy, is based on the Boost-Buck converter architecture; the cascade process is achieved by a step-up and step-down converter. The Cuk converter's circuit diagram, which operates in two stages, is shown in Fig. 1.

When operating in mode 1, the controller will be in the ON position. The supply voltage charges the inductor with energy at this time, and diode D transforms the reverse bias before being turned off. The regulator is running in mode 2, the diode D1 is biased acceleratively, and the capacitor C1 is charged to L1, D1, and Vs.

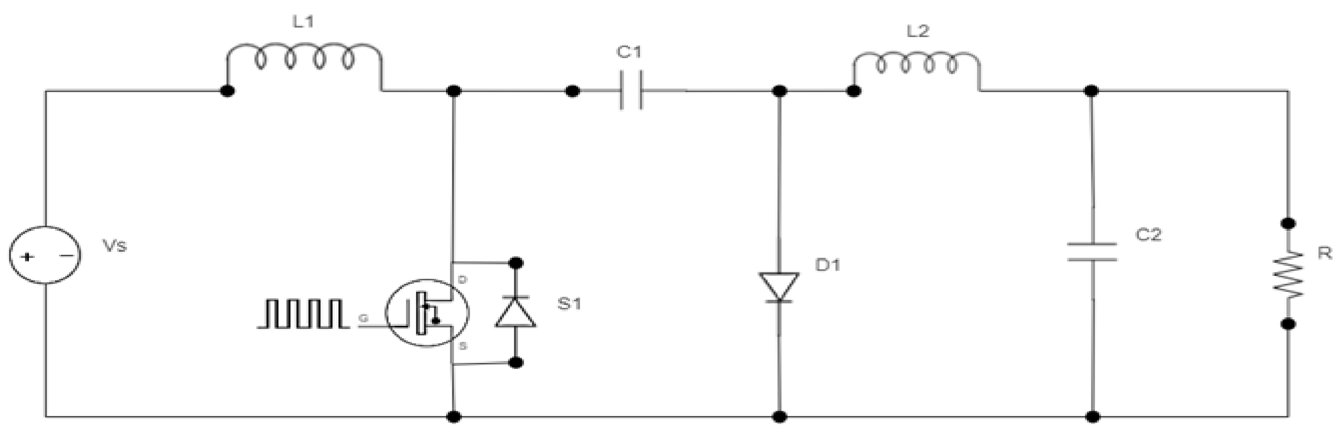

Fig. 1 Cuk Converter

Capacitor C1 discharges to capacitors C0 and L2 as well as the load. The inductor's stored energy will now be transmitted to the load.

Voltage across L_1

$$V_{in}DT + (V_{in} - V_{C1})(1 - D)T = 0 \quad (1)$$

$$V_{in}(1 - D)V_{C1} = 0 \quad (2)$$

$$V_{C1} = \frac{V_{in}}{1-D} \quad (3)$$

Voltage across L_2

$$(V_0 + V_{C1})DT + V_0(1 - D)T = 0 \quad (4)$$

$$V_0 + DV_{C1} = 0 \quad (5)$$

$$V_0 = -DV_{C1} = -\frac{DV_{in}}{1-D} \quad (6)$$

Using C2 as a balancer allows inductor current to flow

$$I_{L2} + I_0 = 0 \quad (7)$$

$$I_{L2} = -I_0 = -\frac{V_0}{R} = \frac{D}{1-D}\frac{V_{in}}{R} \quad (8)$$

The power balancing equation is

$$V_{in}I_{L1} = V_0 I_0 = \frac{v_0^2}{R} = \frac{D^2}{(1-D)^2}\frac{V_{in}^2}{R} \quad (9)$$

$$I_{L1} = \frac{D^2}{(1-D)^2}\frac{V_{in}}{R} \tag{10}$$

Although it generates an inverted output, this converter performs similarly to a buck and boost converter. It consists of two operational phases. The Landsman Converter's mode 1 functioning is shown in Fig. 2. When the regulator operates in mode 1, the capacitor is charged, the voltage Vs biases the diode, and the inductors L 2 and L 1 are turned on.

Calculation of the voltage and current ripple.

$$I_{L1MAX} = I_{L1MIN} + \frac{DV_{in}T}{L_1} \tag{11}$$

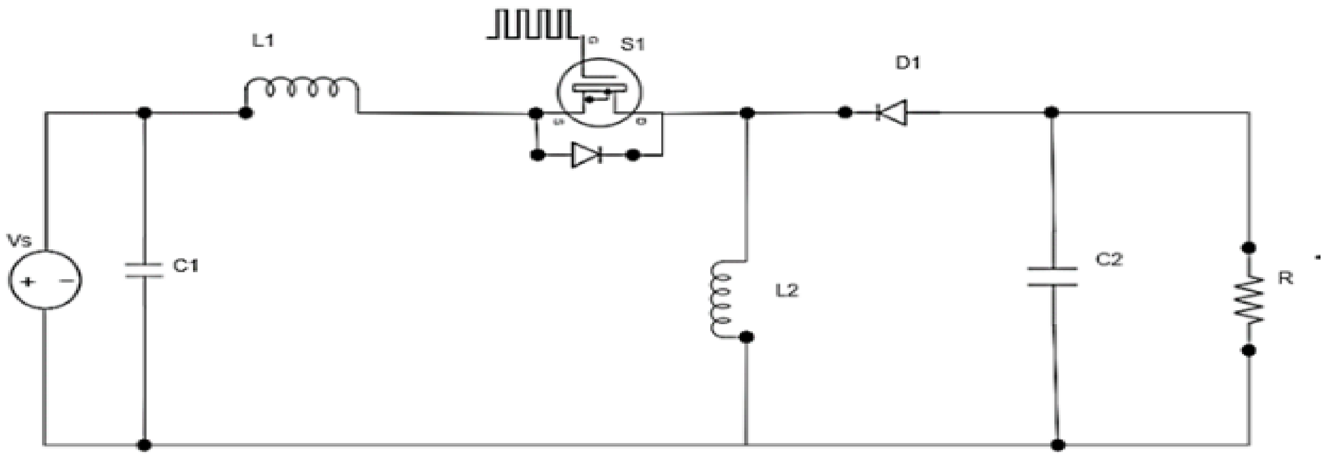

Fig. 2 Circuit Diagram of Landsman converter

$$\hat{I}_{L1}\big|_{p-p} = I_{L1MAX} - I_{L1MIN} = \frac{DV_{in}T}{L_1} \tag{12}$$

From the equation $I_{L1,}$ consider D = S,

$$I_{L1MAX} + I_{L1MIN} = 2I_{L1} = \frac{2S}{(1-S)^2}\frac{V_{in}}{R} \tag{13}$$

$$I_{L1MAX} = \left[\frac{S}{(1-S)^2} + \frac{RT}{2L_1}\right]\frac{SV_{in}}{R} \tag{14}$$

$$I_{L1MIN} = \left[\frac{D}{(1-S)^2} - \frac{RT}{2L_1}\right]\frac{SV_{in}}{R} \tag{15}$$

$$I_{L2MAX} = I_{L2MIN} - \frac{V_0}{L_2}(1-S)T = I_{L2MIN} + \frac{V_{in}}{L_2}ST \tag{16}$$

$$\hat{I}_{L2}\big|_{p-p} = I_{L2MAX} - I_{L2MIN} = \frac{SV_{in}T}{L_2} \tag{17}$$

To calculate voltage ripples

$$v_{c1} = \frac{1}{c1}\int_0^{ST} i_{c1}dt \tag{18}$$

The condition $0 < t \leq ST$ $\qquad i_{c1} = i_{L2}$

$$\frac{1}{c1}\int_0^{ST} i_{c1}dt = \frac{1}{c1}\int_0^{ST} i_{L2}dt \tag{19}$$

$$\hat{v}_c = \frac{1}{c1}x\frac{1}{2}x\frac{T}{2}x\frac{V_{in}ST}{2L_2} = \frac{V_{in}ST^2}{8L_2C_2} \tag{20}$$

3. Proposed Converter design

The simple converter circuit contains a single adder low pass filter, which is the simplest and produces high ripple output. And also, the converter should contain both input current and output current to be continuous. However, all of the converters' input or output currents will often be constant. This study creates continuous currents for input and output using a hybrid system. The Cuk converter and Landsman converter (HCLC) are combined to create a continuous input and output current. The Cuk converter functions on continuous input and discontinuous output, implying the output will suddenly change like a pulse or regularly hit zero. This variation makes discontinuous output, but the Landsman converter works on discontinuous input and continuous output. Hence the combination of the Cuk converter and Landsman converter make both the input and output continuous.

The hybrid converter topology is depicted in figure 3. It has a main switch S_1(MOSFET), two inductors L_1 and L_2, four capacitors C_1, C_3 and C_4, an output capacitor C_2, three diodes D_1 and D_2, an output diode D_0. Pulse Width Modulation is employed to control switches. All functions of the switches will have the same duty cycle [22].

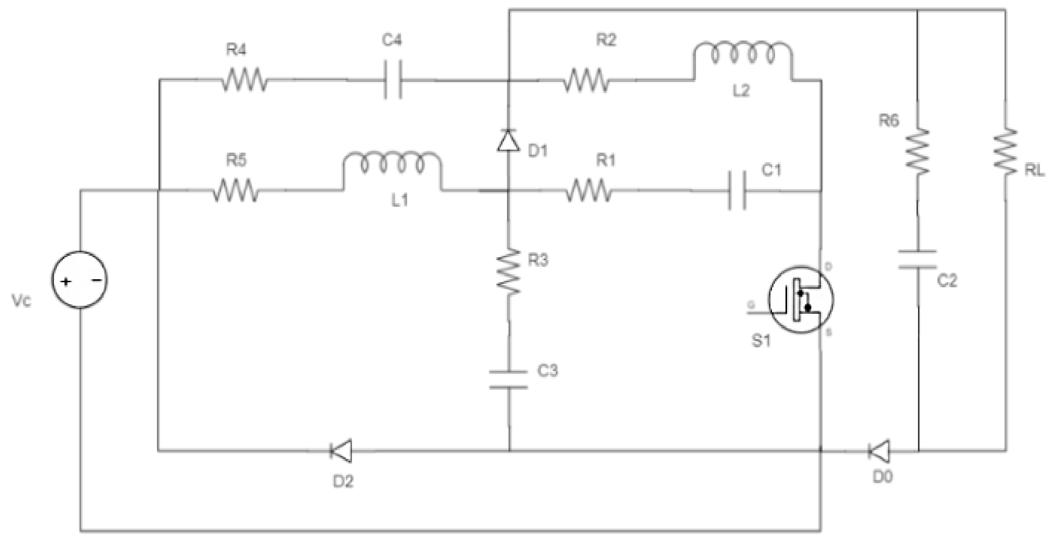

Fig. 3 Proposed hybrid converter circuit

3.1. Working operation of the hybrid converter

In order to function flawlessly, the HCL converter is required to operate in both shoot-through and non-shoot-through modes (0 to DT_s), where D is the duty cycle ratio. The proposed converter uses continuous conduction, starting with all inductances (L1 and L2) demagnetized and all capacitances (C1, C2, C3 and C4) fully charged.

3.1.1. Mode 1 (shoot-through mode)

When the switch S1 is ON condition in mode 1 Inductor will get charged, and the diode will be forward biased, and when the capacitors C_1 gets charges, the capacitors C_2, C_3 are C_4 discharges and diodes D_2 and D_0 performs reverse bias. The current path in this circuit loop is $(V_c - R_5 - L_1 - D_1 - R_2 - L_2 - S_1 - V_c)$ displays in Fig. 4(a).

3.1.2. Mode 2 (non-shoot through mode)

When switch S1 is OFF condition in mode 2 Inductor will release energy to the diode D1, which will perform the reverse bias and when the capacitors C_1 gets discharged, the capacitors C_2, C_3 are C_4 discharged and diodes D_2 and D_0 performs forward bias. For this mode, the current path is $(V_c - R_5 - L_1 - R_3 - C_3 - D_2 - R_4 - C_4 - R_6 - C_2 - D_0 - V_c)$ shown in Fig. 4(b).

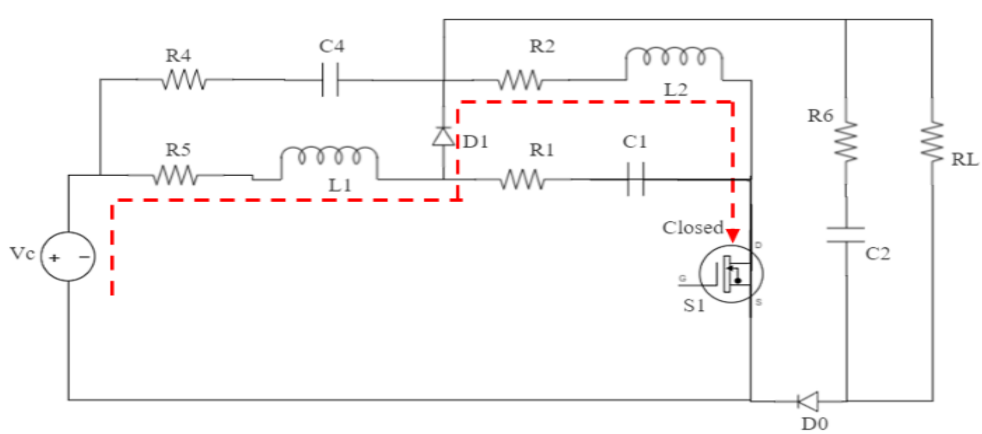

Fig. 4(a) Shoot through

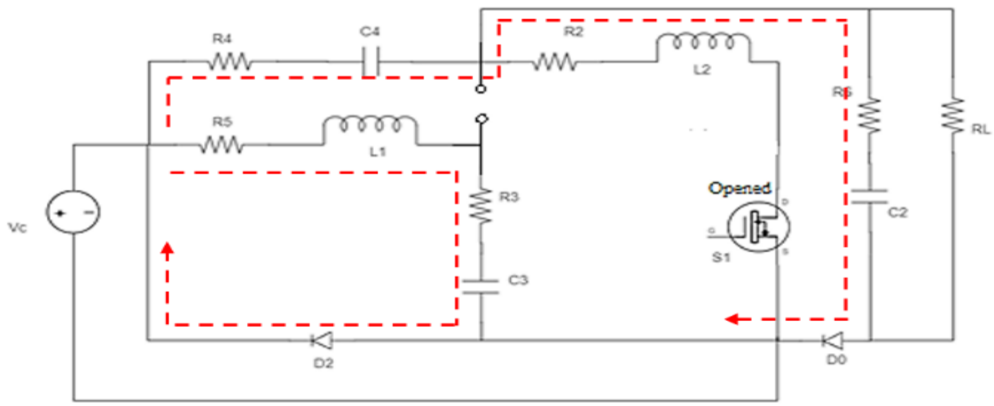

Fig. 4 (b) Non-Shoot through

4. Mathematical Expressions

4.1. Voltage gain calculation

By controlling the switch, we can get voltage equations for shooting and non-shooting. The source voltage (V_c) is determined by changing the switch state S_1 .

The equation is ($V_c = V_{in}$)

Shoot equation (23) can be expressed as below,

$$V_{in} - V_{L_1} - V_{L_3} - 2V_d = 0 \quad (21)$$

$$V_{in} - V_{C_4} - V_{L_2} - V_{C_1} - 4V_d = 0 \quad (22)$$

$$V_{C_2} - V_d = -V_0 \quad (23)$$

Non-shoot equation (24) can be expressed as below,

$$V_{in} - V_{C_4} - V_{L_2} - V_{C_1} - V_{L_1} - V_0 - 4V_d = 0 \quad (24)$$

Using the voltage second balance law on an inductor L_1,

$$(V_{in} - V_{C_3} - 2V_d)D + (V_{in} - V_{C_4} - V_{C_1} - V_0 - 4V_d)(1-D) = 0 \quad (25)$$

After rearranging the previous equation:

$$V_0 = \frac{V_{in} - V_{C_1}D + V_d(2D-4)}{(1-D)} - V_{C_4} \quad (26)$$

Induced voltage across both inductors can be calculated as follows since both inductors L1 and L2 are identical:

$$V_{L_2} = V_{L_1} = \frac{V_{C_1} + V_{C_2} + V_0 - 4V_d}{2} \quad (27)$$

$$(V_{C_1} - 7V_d)D + \left(\frac{V_{C_1} + V_{C_2} + V_0 - 4V_d}{2}\right)(1-D) = 0 \quad (28)$$

$$V_{C_1} = -\left(\frac{1-D}{1+D}\right)V_0 + \left(\frac{10D+4}{1+D}\right)V_d \quad (29)$$

Using the voltage second balance law on an inductor $L_2$and L_1

$$(V_{C_4} + V_{C_2} + V_0 - 4V_d)D + \left(\frac{V_{C_1} + V_{C_2} + V_0 - 4V_d}{2}\right)(1-D) = 0 \quad (30)$$

$$V_{C_4} = \frac{-V_0(D+1) + V_{C_1}(D+1) + 4V_d(1+D)}{2D} \quad (31)$$

$$V_{C_4} = -\left(\frac{D+1}{2D}\right)V_0 + \left(\frac{D+1}{2D}\right)V_{C_1} + \left(\frac{D+1}{2D}\right)4V_d \quad (32)$$

From equations (30) & (32), equation (26) can be written as below. Under circuit component ideal condition V_d=0, and the proposed converter's output voltage is given by,

$$\frac{V_0}{V_{in}} = \left(\frac{1+2D}{1-D}\right) \quad (33)$$

$$V_0 = \left(\frac{1+2D}{1-D}\right)V_{in} \quad (34)$$

According to equation (30), the boost mode will operate only in the duty ratio cycle, and that is the proposed hybrid converter.

4.2. Design of passive components

The inductors and capacitors are crucial passive parts in the converter design. Some assumptions must be made to ensure that the converter performs in the rated condition:

Both the inductors have identical values, with the present slew rate di/dt is 0.1 A/μs.

$$C_1 \geq \frac{I_0(1-D)}{f_s \Delta V_{rC_1}} \quad (35)$$

$$C_2 \geq \frac{I_0(1-D)}{f_s \Delta V_{rC_2}} \quad (36)$$

$$C_3 \geq \frac{I_0(1-D)}{f_s \Delta V_{rC_3}} \quad (37)$$

$$C_4 \geq \frac{I_0(1-D)}{f_s \Delta V_{rC_4}} \quad (38)$$

where $V_{rC_1}, V_{rC_2}, V_{rC_3}$ *and* V_{rC_4} are the voltage ripples of capacitor C_1, C_2, C_3 *and* C_4 and. The two inductors' values, L_1 and L_2, are made equal, which are determined by the following equation:

$$L_1 = L_2 = \frac{V_i}{di/dt} = \frac{(1-D)V_0}{(1+2D)di/dt} \quad (39)$$

This proposed converter will achieve better voltage gain with a reduced smooth switching and duty cycle.

5. Experimental Results

With the help of MATLAB, the proposed HCLC performance is tested by the simulation based on the parameters and components mentioned before, given Table 1 displays the specifications. The simulation results for the prototype converter are shown in Fig. 5.

Table 1. System parameters for the proposed HCL converter

Sl. No	Element	Specifications
1	Input voltage (V_{in})	90 V
2	Capacitor	$63\mu F$
3	Inductor	1.9mH
4	Resistor	5.76Ω
5	Switching Frequency	50KHz
6	Duty ratio	0.7

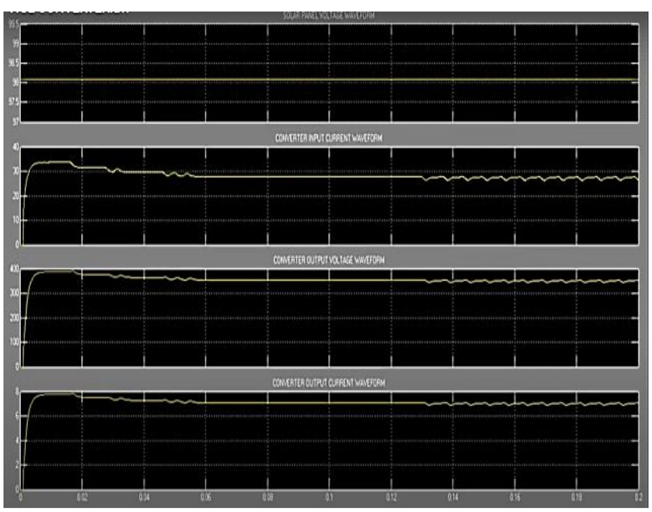

Fig. 5 (a) Solar input voltage (b) Converter input current (c) Output voltage Converter (d) Output current Converter

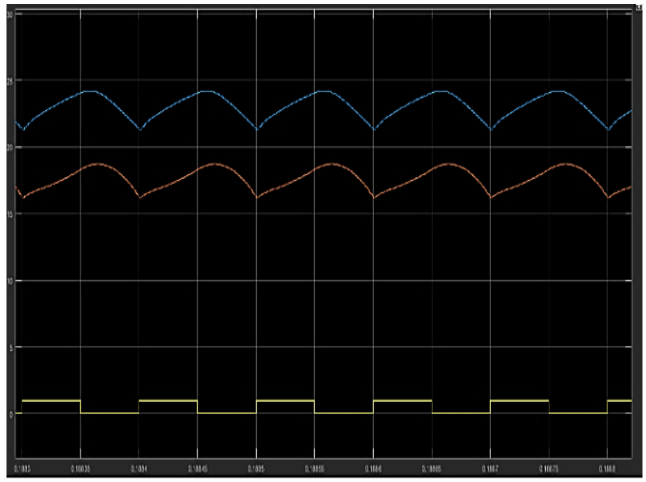

Fig. 6 Inductor's current

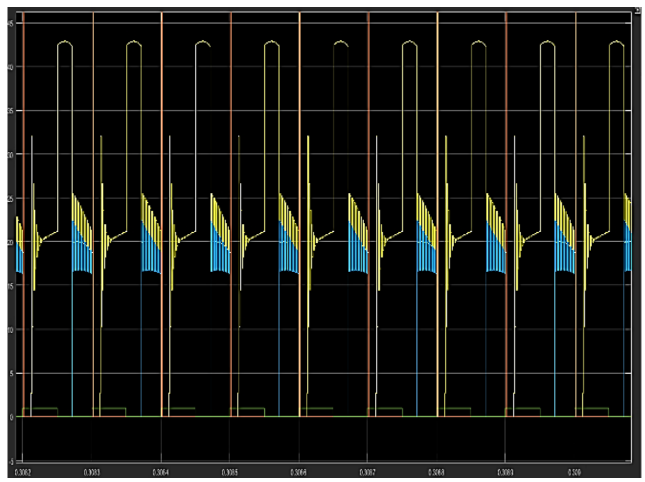

Fig. 7 Diode current

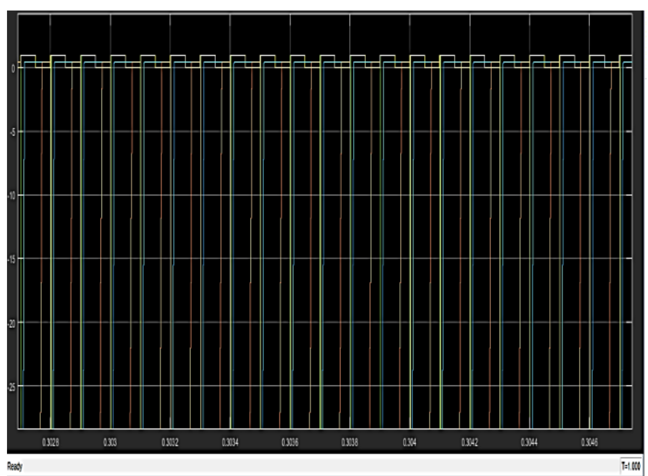

Fig. 8 Diode voltage

A 90V input voltage and a 0.7 duty cycle will result in an output voltage of 355V. The voltage drop across the switch, diodes, capacitors, and inductors will effectively limit the voltage gain.[18] Fig. 5(a) displays the input voltage of the recommended converter, Fig. 5(b) displays the input current, Fig 5(c) displays the output voltage, and Fig 5(d) displays the output current (d). Fig 6 displays the hypothetical HCL converter's inductor current. Fig. 7 displays the diode current of the proposed HCL converter. Fig. 8 displays the projected diode voltage of the HCL converter.

The HCL converter and the current converter are contrasted in Table 2.

The maximum gain during 0.5 D1 is achieved by the HCL converter, whereas the other converters do not. The HCL converter has 10 parts, one of which is a switch.[15] There are eight components in the quadratic boost converter shown in [10] [11], but it yields less gain than the HCL converter. One switch is used by the converter in [10], while the converter in [11] uses two switches. Since it employs fewer components than the conventional landsman converter, the HCL offers greater conversion than prior systems [14]. More capacitors and inductors are used in the converter in [9].

Table 2. Analysis of proposed and existing converters in comparison

Components	Converters						
	Reference [9]	Referen ce [10]	Reference [11]	Buck-Boost [13]	Cuk [14]	Landsman [16,17]	Proposed HCLC
Switch S	1	1	2	1	1	1	1
Inductor L	1	2	2	2	2	3	2
Capacitor C	5	2	2	2	2	3	4
Diode D	5	3	2	1	1	3	3
Voltage gain (Where D=S)	$\frac{3}{(1-S)} \times \frac{1+S}{1+S}$	$\frac{1}{(1-S)^2} \times \frac{1+S}{1+S}$	$\frac{1}{(1-S)^2} \times \frac{1+S}{1+S}$	$\frac{-S}{(1-S)} \times \frac{1+S}{1+S}$	$\frac{-S}{(1-S)} \times \frac{1+S}{1+S}$	$\frac{-(1+S)}{(1-S)} \times \frac{1+S}{1+S}$	$\left(\frac{1+2S}{1-S}\right) \times \frac{1+S}{1+S}$
No. of total devices	12	8	8	6	6	10	10

Up to gain 13 are produced with a 0.8 duty cycle. Fig. 9 displays the specifications for the voltage gain of the planned HCL converter. Furthermore, after a 90% duty ratio, the voltage gain curve of the proposed HCL converter starts to expand exponentially.[19] For instance, the suggested HCL converter produces 355V output voltage from 90Vof input voltage, which results in the 98.61%efficiency. Additionally, the HCL converter's switching stress is typically lower than that of supporters of quadratic increase.

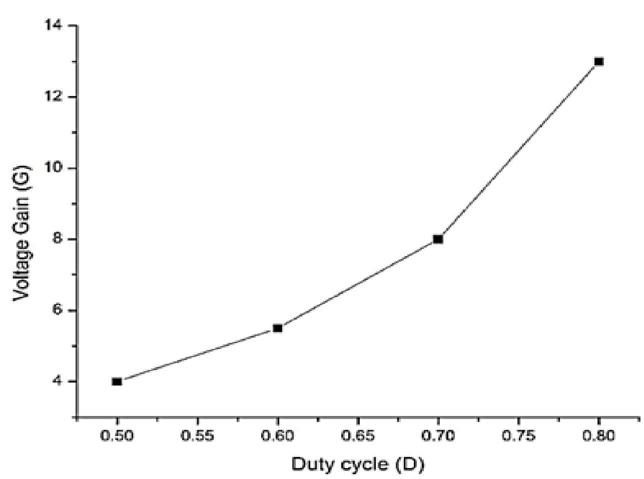

Fig. 9 Performance of Voltage gain in the proposed converter

6. Conclusion

The research results in high efficiency and high voltage gain in a hybrid DC-DC converter using a single switch. The Cuk and Landsman apostles were combined to suggest a topology. A high voltage gain switch produces a non-inverting output through continuous input current mode. The proposed architecture offers a considerable voltage gain compared to current Cuk and Landsman converters. It was carefully examined how the hybrid converter operates and how it is designed. Validation tests were conducted utilizing converter privileges, voltage gain, and circuit modelling study components. In addition to providing a high voltage conversion ratio, semiconductor components are stressed at low voltages, making this converter very efficient. Half-loaded, the system achieves 98.61% efficiency. It is undoubtedly better to use the recommended HCL converter to get high voltage on semiconductors and devices without a lot of voltage. Traditional converters overload semiconductors and devices, while this device provides high voltage without overloading them.

Acknowledgements

The Author, with deep gratitude, would thank the supervisor for his guidance and constant support during this research.

References

[1] Babaei, E., Maheri, H. M., Sabahi, M., and Hosseini, S. H, "Extendable Non-Isolated High Gain DC-DC Converter Based on Active-Passive Inductor Cells," *IEEE Transactions on Industrial Electronics*, vol.65, no.12, pp.9478-9487, 2018.

[2] Müller, L. and Kimball, J.W, "High Gain DC-DC Converter Based on the Cockcroft–Walton Multiplier," *IEEE Transactions on Power Electronics*, vol.31, no.9, pp.6405-6415, 2015.

[3] Lakshmi, M. and Hemamalini, S, "Nonisolated High Gain DC-DC Converter for DC Microgrids," *IEEE Transactions on Industrial Electronics*, vol.65, no.2, pp.1205-1212, 2017.

[4] Choi, H., Ciobotaru, M., Jang, M. and Agelidis, V.G, "Performance of Medium-Voltage DC-Bus PV System Architecture Utilizing High-Gain DC-DC Converter," *IEEE Transactions on Sustainable Energy*, vol.6, no.2, pp.464-473, 2015.

[5] Revathi, B.S. and Prabhakar, M, "Non Isolated High Gain DC-DC Converter Topologies for PV Applications–A Comprehensive Review," Renewable *and Sustainable Energy Reviews*, vol.66, pp.920-933, 2016.

[6] Revathi, B.S. and Mahalingam, P, "Non-Isolated High Gain DC-DC Converter with Low Device Stress and Input Current Ripple," *IET Power Electronics*, vol.11, no.15, pp.2553-2562, 2018.

[7] Dr J.Gnanavadivel, M.Shunmathi, P.Muthu Thiruvengadam, S.Narthana, "Analysis of DC-DC Converter with High Step-Up Gain for Alternative Energy Sources," International Journal of Engineering Trends and Technology, vol.69, no.4, pp.162-168, 2021. Crossref, Https://Doi.Org/10.14445/22315381/IJETT-V69I4P223.

[8] Infenshirley, M., Et Al, "Design of Fuzzy Controller for PV Solar Plant As STATCOM (PV-STATCOM) To Mitigate SSR." International Journal of Engineering Trends and Technology, vol.70, no.4, pp.389-402, 2022. Crossref, Https://Doi.Org/10.14445/22315381/IJETT-V70I4P234

[9] Chen, M., Li, K., Hu, J. and Ioinovici, A, "Generation of A Family of Very High DC Gain Power Electronics Circuits Based on Switched-Capacitor-Inductor Cells Starting From A Simple Graph," *IEEE Transactions on Circuits and Systems I: Regular Papers*, vol.63, no.12, pp.2381-2392, 2016.

[10] Appathurai, A., Carol, J. J., Raja, C., Kumar, S. N., Daniel, A. V., Malar, A. J. G., ... and Krishnamoorthy, S, "A Study on ECG Signal Characterization and Practical Implementation of Some ECG Characterization Techniques," *Measurement*, vol.147, pp.106384, 2019.

[11] Li, K., Hu, Y. and Ioinovici, A,"Generation of the Large DC Gain Step-Up Nonisolated Converters In Conjunction with Renewable Energy Sources Starting From A Proposed Geometric Structure," *IEEE Transactions on Power Electronics*, vol.32, no.7, pp.5323-5340, 2016.

[12] Wang, F, "A Novel Quadratic Boost Converter with Low Current and Voltage Stress on Power Switch for Fuel-Cell System Applications," Renewable *Energy*, vol.115, pp.836-845, 2018.

[13] Lu, Y., Wu, H., Sun, K. and Xing, Y,"A Family of Isolated Buck-Boost Converters Based on Semiactive Rectifiers for High-Output Voltage Applications," *IEEE Transactions on Power Electronics*, vol.31, no.9, pp.6327-6340, 2015.

[14] Malar, J. G., & Kumar, C. A, " Implementation of Mppt Techniques for Wind Energy Conversion System," *Internal Journal of Research and Analytical Reviews*, vol.5, no.3, 2018.

[15] Maroti, P.K., Padmanaban, S., Bhaskar, M.S., Blaabjerg, F. and Wheeler, P, "New Inverting Modified CUK Converter Configurations with Switched Inductor for High-Voltage/Low-Current Renewable Applications," *In 20th European Conference on Power Electronics and Applications (EPE'18 ECCE Europe)* (pp.P-1). IEEE.

[16] Norbert Njuanyi Koneh, Jae-Sub Ko, Dae-Kyong Kim, "Characteristics of An AC/DC Hybrid Converter According To Load Fluctuation," International Journal of Engineering Trends and Technology, vol.69, no.11, pp.205-210, 2021, Crossref, Https://Doi.Org/10.14445/22315381/IJETT-V69I11P226.

[17] Prodic, A., Maksimovic, D. and Erickson, R.W, "Design and Implementation of A Digital PWM Controller for A High-Frequency Switching DC-DC Power Converter," *In IECON'01. 27th Annual Conference of the IEEE Industrial Electronics Society* (Cat. no.37243) vol.2, pp.893-898, 2001.

[18] Malar, A. J. G., Kumar, C. A., and Saravanan, A. G," IOT Based Sustainable Wind Green Energy for Smart Cites Using Fuzzy Logic Based Fractional Order Darwinian Particle Swarm Optimization," *Measurement*, vol.166, pp.108208, 2020.

[19] Abdel-Rahim, O. and Wang, H., "A New High Gain DC-DC Converter with Model-Predictive-Control Based MPPT Technique for Photovoltaic Systems," *CPSS Transactions on Power Electronics and Applications*, vol.5, no.2, pp.191-200, 2020.

[20] Shadmand, M. B., Mosa, M., Balog, R. S., and Rub, H. A, "An Improved MPPT Technique for High Gain DC-DC Converter Using Model Predictive Control for Photovoltaic Applications," In *IEEE Applied Power Electronics Conference and Exposition-APEC 2014*, pp.2993-2999, 2014.

[21] Kavita Joshi, Vaishali Raut, Surendra Waghmare, Manisha Waje, Rupali Patil, "Maximum Power Operation of A PV System Employing Zeta Converter with Modified P&O Algorithm," *International Journal of Engineering Trends and Technology*, vol.70, no.7, pp.348-354, 2022. Crossref, Https://Doi.Org/10.14445/22315381/IJETT-V70I7P236

[22] Singh, P.K., Singh, B., Bist, V., Al-Haddad, K. and Chandra, A. "BLDC Motor Drive Based on Bridgeless Landsman PFC Converter with Single Sensor and Reduced Stress on Power Devices," *IEEE Transactions on Industry Applications*, vol.54, no.1, pp.625-635, 2017.

[23] Sivasankari, B., Ahilan, A., Jothin, R., and Malar, A. J. G. "Reliable N Sleep Shuffled Phase Damping Design for Ground Bouncing Noise Mitigation," *Microelectronics Reliability*, vol.88, pp.1316-1321, 2018.